

ACA048737

B.S.

DDC
RECEIVED
JAN 17 1978
R
Q7D

technical information from



Rockwell International

DISTRIBUTION STATEMENT A

Approved for public release;
Distribution Unlimited



ACCESSION NO.	
NTIC	Library Section <input checked="" type="checkbox"/>
DDC	Doc. Section <input type="checkbox"/>
UNANNOUNCED	<input type="checkbox"/>
JUSTIFICATION	
BY	DISTRIBUTION/AVAILABILITY CODES
Dist.	AVAIL. CODE OR SPECIAL
A	

⑥ AN ELECTRICAL SURGE ARRESTOR (ESA) MODEL FOR ELECTROMAGNETIC PULSE ANALYSIS

⑮ F04704-76-C-0008

⑪ 27 September 1977

⑫ 8p.

⑩ by C. T. Kleiner, E. D. Johnson, J. R. McMurray and F. T. Suzuki

Presented to

IEEE Transactions on Nuclear Science
December 1977

THE DISTRIBUTION OF THIS REPORT
IS UNLIMITED



Rockwell International

Autonetics Group
3370 Miraloma Avenue
P.O. Box 4182
Anaheim, California 92803

DDC
RECEIVED
JAN 17 1978
RECEIVED

⑭ X77-958/561

390 713

Handwritten initials or signature.

**AN ELECTRICAL SURGE ARRESTOR (ESA) MODEL FOR
ELECTROMAGNETIC PULSE ANALYSIS***

C. T. Kleiner, E. D. Johnson, L. R. McMurray and F. T. Suzuki
Rockwell International Electronics Operations, Anaheim, CA 92803

I. SUMMARY

Electrical Surge Arrestors (ESA's) have been used extensively for lightning and EMP protection. These components are characterized by (a) presenting an open circuit (high impedance) below the gap breakdown potential, (b) becoming a virtual short-circuit above the gap breakdown and (c) displaying a significantly higher level of apparent gap breakdown for very fast input voltage rise-times (dv/dt). This paper describes a mathematical model for a spark gap surge arrester which has been used successfully to characterize ESA response to the following stimulus:

1. Below DC Gap Breakdown
2. At or above Gap Breakdown
3. At high apparent Gap Breakdown voltage as a function of increased rise-time
4. Damped Sinewave Input (below and at Gap Breakdown)
5. Exposed to prompt gamma radiation using a Flash X-Ray source and an electrical input

II. MODEL PARAMETERS AND EQUATIONS

Figure 1 illustrates the equivalent circuit for the Electrical Surge Arrester model. The linear portion of the model is defined by the L, R_{PL}, C_S and C_G elements. The nonlinear characteristics of the model is illustrated in Figure 2, and basically represents the complex reaction of initial streamer/arc formation followed by plasma formation and includes the Thermionic potential observed during the ON or conduction phase of ESA operation. The various model parameters, nonlinear equations which utilize the parameters will be defined and illustrated by model application and comparison to test results. The various test circuits are also shown for the benefit of other investigators wishing to characterize ESA's in a manner described herein.

Definition of Model Parameters and Equations

1. Linear Section

- L = Lead Inductance (usually in nano henries)
- R_{PL} = Flux loss ("Q") associated with L (usually in K ohms)
- C_S = Stray Capacitance (reflected capacitance at the ESA terminals from all other sources, leads, etc.)
- C_G = Gap Capacitance (measured or calculated for the Gap)

*This work was performed on the Wing VI In-Place EMP Program, Air Force Contract F04704-78-C-0008, under the direction of SAMSO (MNNH) Project Officer Captain R. I. Lawrence.

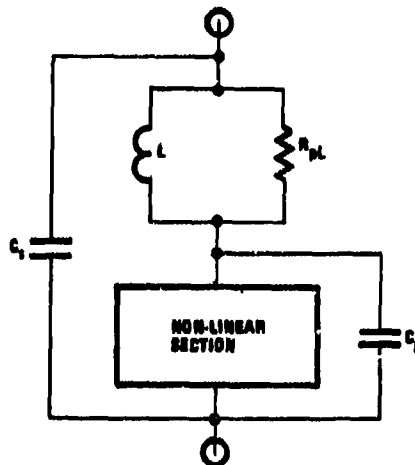


Figure 1. Electrical Surge Arrester (ESA) Model

2. Nonlinear Section

- (a) R_g = A nonlinear resistor dependent on the energy being dissipated within the gap and transferred to the surrounding medium

Equations:

$$R_g = \frac{K_1}{W} \quad (1)$$

$$W = W_{IN} - W_{OUT} \quad (2)$$

$$W_{IN} = \int \left[\frac{V_g^2}{R_{gn-1}} + |V_g| \cdot I_g \right] dt \quad (3)$$

$$W_{OUT} = \int \frac{W}{\tau_d} dt \text{ or } \int P_{m1} dt; \quad (4)$$

(whichever is less)

where:

- R_g = Instantaneous Resistance of the gap (ohm)
- V_g = Instantaneous Voltage across the gap (volts)
- I_g = Instantaneous Current through the gap (amps)
- W = Instantaneous Energy in the gap (joules)
- W_{IN} = Instantaneous Energy generated as input to the gap (joules)

- W_{OUT} = Instantaneous Energy removed from the gap to the surrounding medium (joules)
- K_1 = Scale factor relating R_g to W (-joules)
- P_{ml} = Maximum instantaneous power lost to the surrounding medium (watts)
- d = Dissipation time constant (an average thermal time constant for establishing the rate at which heat energy (joules) is dissipated to the surrounding medium) (sec)
- R_{gmax} = Maximum resistance of the air gap (ohms)
- R_{gmin} = Minimum resistance of the air gap (ohms)
- W_{min} = Minimum energy in the air gap (joules)

The following controls are employed:

- No. 1 If $V_g \geq V_{DC}$ and $W \geq 0$, then initiate timer at t_0 (time at which the condition for streamer formation has been achieved)
- No. 2 At $t = t_0 + \tau_{GF}$ initiate computation of W and subsequent modification of R_g (see Figure 2 characteristic curve)
- No. 3 Continue to monitor W until $W \leq W_{min}$. Also monitor R_g and limit R_g to R_{gmin} by comparing $R_g(W)$ to R_{gmin}
- No. 4 Return R_g to R_{gmax} when gap is fully extinguished $I_g \leq I_{gmin}$

(b) Thermionic Effect = The phenomenon that accounts for the high ON voltages observed in ESA's (over 100 volts), whereby the emitting ESA block effectively becomes a cold cathode, while the collecting ESA block becomes the plate, in what is essentially Thermionic reaction, namely, the plasma creates a junction which is represented mathematically by the following equations:

$$I_{RF1} = I_{S1} (\exp VR/M_1 \theta) - 1 \quad (5)$$

$$I_{RF2} = I_{S2} (\exp -VR/M_2 \theta) - 1 \quad (6)$$

where:

V_R = Thermionic junction potential (volts)

I_{S1}, I_{S2} = A pseudo-saturation current for the Thermionic Rectifier (and are also functions of temperature and effective plasma area)

M_2, M_2 = Multiplier for empirical fit (M has a range of 50 to 500 depending on the particular ESA) (non-dimensional)

In addition, there is a slight tendency for these "Thermionic Rectifiers" to "store" charge similar to a semiconductor rectifier, hence, the net current in each Thermionic Rectifier is formulated as follows:³

$$I_{R1} = I_{RF1} + R I_{RF1} \quad (7)$$

$$I_{R2} = I_{RF2} + R I_{RF2} \quad (8)$$

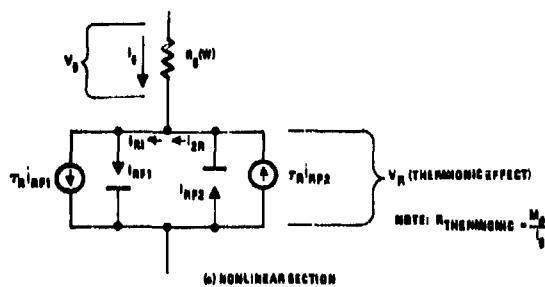
where:

τ_R = Thermionic electron recombination time (which is believed to be on the order of a few nanoseconds)

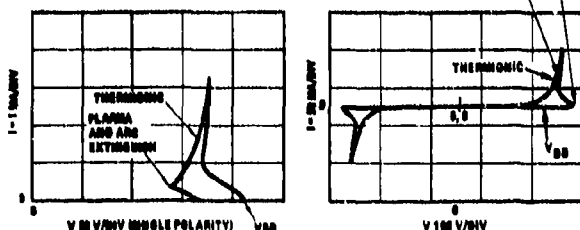
$$\theta = kT/q = .026 @ 27^\circ C \quad (T \text{ is set at } 300^\circ K) \quad (9)$$

A set of typical ESA model data (Antenna ESA) is shown in Table I.

Although the model accounts for numerous nonlinear effects, it nevertheless is a very simple conceptual representation of the phenomenon that can be attributed to spark gap ignition and plasma's in general.⁴ The next section will show how a particular Electrical Surge Arrestor was



(a) NONLINEAR SECTION



(b) LOW FREQUENCY I vs V CHARACTERISTICS OF (a)

Figure 2. Non-Linear Section and DC Characteristics

- V_{DB} = Gap breakdown threshold voltage (volts)
 V_{DB} 100KV/inch in air at STP
- τ_{SF} = Time for Streamer Formation (τ_{SF} increases with gap width)
- i = Current generated across the gap as a function of γ (γ = generation rate and A_0 = effective area)
- I_{gmin} = Instantaneous value of arc current below which the arc extinguishes.

characterized and tested to validate the subject model.

III. ESA CHARACTERIZATION

Although several types of ESA's were modeled and characterized (Audio, Power and Antenna ESA's), the lower power device (Joslyn Part No. 27-10425-11) was selected for presentation here since it was also characterized for the effects of a prompt gamma pulse produced by a 2-MEV Flash X-ray. This test was performed to determine if the presence of a prompt gamma pulse would effectively aid ESA firing and hence, tend to lower the effect of high coincident dv/dt inputs (or ESG overshoot) without lowering the ON voltage. This was found to be the case and is believed to be the first published data on this effect. The device was characterized for both the linear and nonlinear components of the model.

Table I. Typical ESA Data

	Parameter	Values	Units	
Linear Section	L	130	nh	
	R_{pL}	2400	ohms	
	C_G	3.18	pf	
	C_S	1	pf	
	K_1	10^{-3}	ohm-Joules	
	P_{m1}	1800	Watts	
	τ_d	.1	usec	
	R_{gmax}	10^{12}	ohms	
	R_g	R_{gmin}	.1	ohms
		W_{min}	10^{-10}	Joules
V_{DB}		185	Volts	
τ_{GF}		1	nsec	
I_{gmin}		5	ma	
Thermionic	I_s	1	ua	
	M	800	-	
	τ_R	.1	nsec	

The linear characteristics can be obtained quite readily by using a network analyzer and solving for the values of L, C_G , C_S , and R_{pL} . The result is shown in Figure 3.

The nonlinear characteristics are considerably more difficult to obtain.

The following tests were conducted to obtain the nonlinear characteristics:

1. Sawtooth Oscillator Test

The first test that can be performed is shown in Figure 4 where the ESA is used as the nonlinear element which produces a sawtooth oscillation. Resistor, R_1 , must be sufficiently large so that the 'holding current' will not sustain a very low electron leakage and prevent oscillation. This determines one of the critical parameters, namely, the minimum power to sustain the arc. This may not be the minimum power required to completely describe the interaction of the plasma with the surrounding medium however.

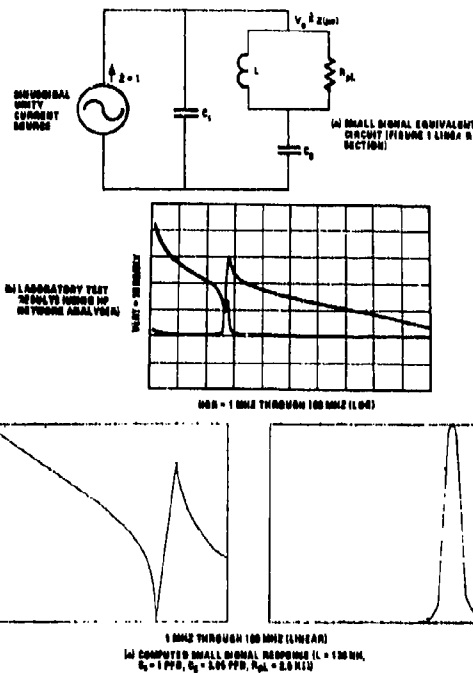


Figure 3. Linear Characterization of the Low Power ESA

The dynamic resistance of the arc can appear quite high even though the capacitor, C_1 is a very low impedance source at the switch point and hence, would be expected to discharge rapidly giving rise to a high current pulse through the ESA; this is not the case for this or other ESA's. The reason for this apparent high discharge impedance in this sawtooth oscillator configuration is postulated to be due to the relatively high resistance of R_{gap} and the relatively high impedance of the onset of the Thermionic conduction $\frac{M\theta}{I_{gap}}$.

2. Fast Rise Time Test

When the ESA is subject to a high voltage, fast rise-time input, two characteristics become apparent. First, the firing potential increases and second, the ON voltage is only somewhat higher than during the sawtooth operation. The dynamic resistance becomes much lower which satisfies the functional relationship between R_{gap} and $M\theta/I_{gap}$ (both resistors being inverse to arc current density). The high dv/dt input results in a voltage breakdown vs rise-time characteristics as shown in Figure 5. There are two regions of the curve which are worthy of discussion. Region I shows a fairly gradual increase in apparent gap breakdown with increasing dv/dt . This increase is attributable to the interaction of the arc formation and energy dissipation coupled with the effect of the reactive linear elements (L's and C's) of the ESA. In Region II the apparent breakdown of the ESA vs dv/dt increased more rapidly. This is attributed to the time required for streamer formation. This occurs prior to arc formation. The net effect of this ESA response to very high values of dv/dt (or high frequency) reduces ESA effectiveness for the high frequency components of EMP. As a result, most ESA's include limiters and low bandpass filters (as shown in Figure 6).

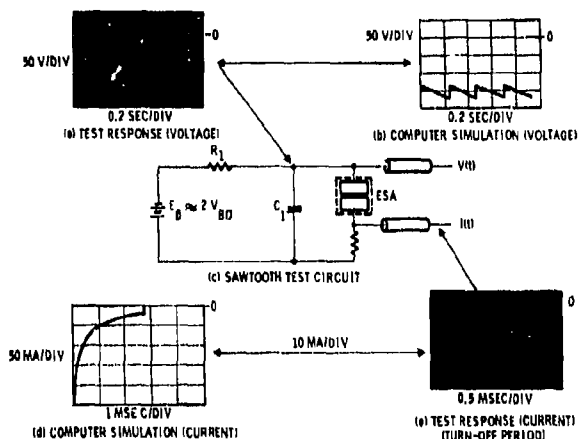


Figure 4. Sawtooth Oscillator Test Results and Comparison to Computer Model Response

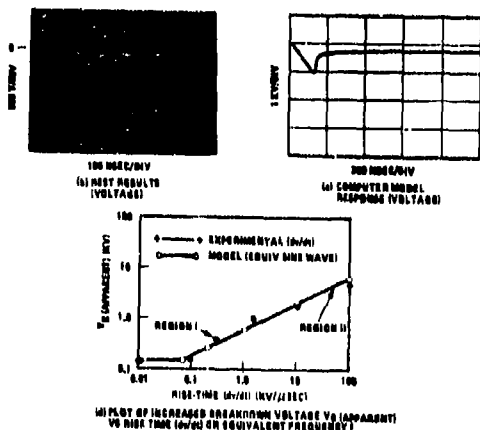
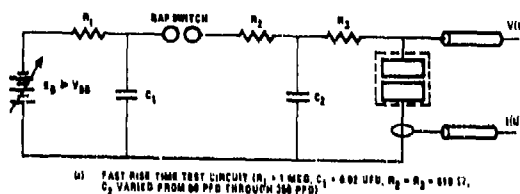


Figure 5. Characterization of Increase in Apparent Voltage Breakdown (or Overshoot) vs Rise Time Test Circuit, Results and Plot of V_B vs dv/dt

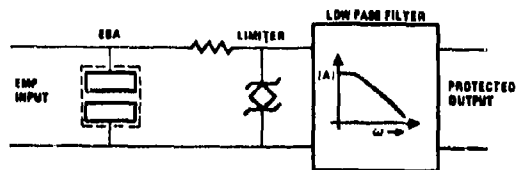


Figure 6. ESA Assembly Including Limiter and Low-Pass Filter

3. Damped Sine Wave Test

In practice a damped sine wave is frequently used to characterize component and/or subsystem response to EMP. As a result, the ESA and corresponding model were also characterized using various damped sine wave input stimulus. The result of this test and model simulation is illustrated in Figure 7. Note that the ESA's can open after the initial shorting if the sustaining energy is insufficient to cause the arc to sustain. This is particularly true for lower frequencies (~1 MHz and below) and "soft" EMP sources.*

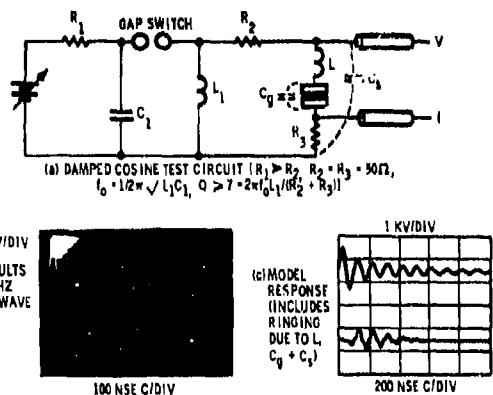
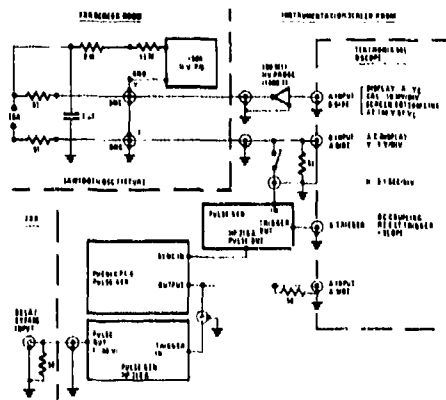


Figure 7. Damped Cosine Wave Test and Comparison

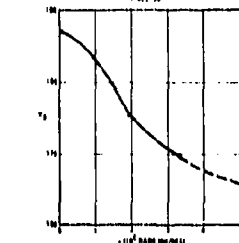
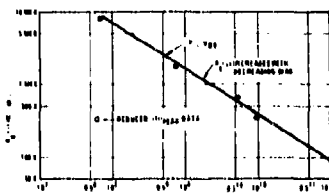
4. Ionization from 2 MEV FXR

In a situation where an antenna ESA can be simultaneously exposed to a high dv/dt pulse and a high $\dot{\gamma}$ pulse, there is a distinct possibility that the ESA may, in fact, be triggered by the $\dot{\gamma}$ pulse (provided of course, that this occurs virtually simultaneously with the EMP pulse). In view of the difficulty associated with synchronizing two short pulses (~20-30 nsec) each from a different source of high intensity EMI, an indirect but correlatable experiment was performed. The approach which was taken utilizes the sawtooth oscillator circuit (shown in Figure 8) as a self-contained EMP source and exposes the ESA unit to $\dot{\gamma}$ using a 2 MEV FXR. This test configuration is shown in Figure 8 with the attendant curves showing decreasing firing potential vs dose rate. From this experiment, it has been possible to characterize the ESA model with the following simple assumption.

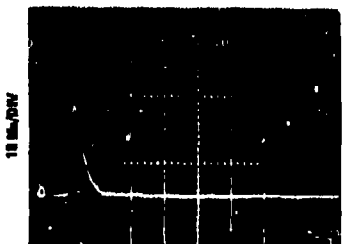
*"Soft" does not necessarily mean "Soft" to EMP or having a low energy content.



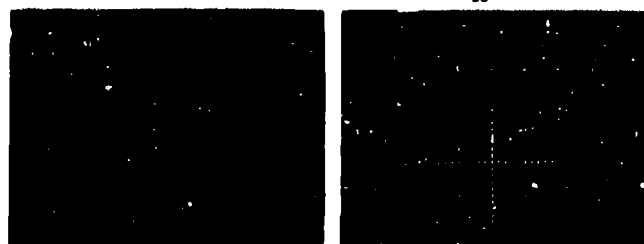
(a) TEST CIRCUIT FOR COMBINED SAWTOOTH OSCILLATOR AND $\dot{\gamma}$ FXR SOURCE $t_p \approx 30$ NSEC



(b) CHARACTERISTICS OF $R_{\dot{\gamma}} + V_{DD}$ vs $\dot{\gamma}$



(c) TEST RESPONSE $R_{\dot{\gamma}}$ vs $\dot{\gamma}$ (PERFORMED ON THE ESA IN A SEPARATE TEST FIXTURE)



(d) TEST RESPONSE V_{DD} vs $\dot{\gamma}$ (TESTED AS SHOWN IN (A))

Figure 8. Test Configuration and Results for Combined Electrical (Sawtooth Oscillator) and $\dot{\gamma}$ (10^8 through 10^{10} R/sec (SI))

The streamer formation is overridden by a minimum energy contributed by the ionizing pulse. This energy was obtained experimentally on two samples and has not been calculated extensively for large sample size types of ESA's. When this energy is exceeded, the conditions for arc formation are enabled and the results for a combined high dv/dt and sufficiently high $\dot{\gamma}$ are shown in Figure 9 for comparison. Of the two samples, one would trigger as low as 10^8 R/sec (SI) while the other required 3×10^8 R/Sec (SI). The exact cause for this wide dispersion is unknown and certainly is indicated worthy of additional investigation. The most significant observation however, indicated that the Thermionic ON voltage seemed virtually unaffected by $\dot{\gamma}$ which is to be expected.

IV. CONCLUSIONS

The ESA model presented in this paper is relatively easy to use (in an appropriate computer program) and permits a detailed evaluation of ESA, Limiter and Filter

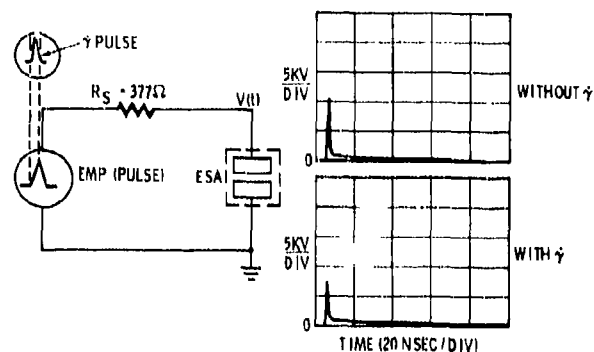


Figure 9. ESA Model Simulation of Combined Fast Rise Time Input and $\dot{\gamma}$ ($>10^8$ R/sec) Comparison

assemblies to a variety of EMP stimulus. The model accounts for the extremely nonlinear behavior of the ESA gap including intermittent firing, variation in ON impedance and other related phenomenon. The model has been more than adequate for EMP assessment and together with other EMP related models permits nonlinear transient response evaluation with minimal run time (on the order of \$10 to \$20 per run using a GFE CDC 7600 computer).

At present, the model does not provide a readily traceable path between ESA device design parameters and the response observed in test or associated with parameter variations. Some of the more subtle parameters of the model appear to have a fairly wide dispersion. Most of these effects are expected to influence the higher frequency components of EMP and should not be significant for well-limited/filtered assemblies using ESA's. Where ESA's stand alone (as protection against lightning), these parameters can be extremely critical; and one could expect to see a wide variation in high frequency response even among the same type and series of ESA's.

At present, the ESA model has been implemented using the SECURE code⁵ which is the baseline software EMP simulation package used for the In-Place EMP program.

V. ACKNOWLEDGMENTS

The authors would like to express their appreciation to Mr. Gene Laport, who conducted the dv/dt experiments and Mr. James T. Blandford, who conducted the 2-MEV FXR experiments. In addition, Mr. G. Page and Mr. R. Fratino provided invaluable review during the process of performing this work. All of the aforementioned individuals are with Electronics Operations of Rockwell.

VI. REFERENCES

1. "EMP" Radiation and Protective Techniques" by: L. W. Ricketts, J. E. Bridges and J. Millett, John Wiley and Sons, Wiley - Interscience Publication, p 161-189.
2. Hart, W. C., and Higgins, D. F., "A Guide to the Use of Spark Gaps for Electromagnetic Pulse (EMP) Protection", Joslyn Electronic Systems, Federal Products Department, Santa Barbara Research Park, P.O. Box 817, Goleta, California. 93017, 1973.
3. Kleiner, C. T., Kinoshita, G., and Johnson, E. D., "Simulation and Verification of Transient Nuclear Radiation Effects on Semiconductor Electronics," IEEE Trans. on Nucl. So. Vol INS-11 No. 5, pp 82-104.
4. Leob, L. B., "The Mechanism of Lightning Discharge", Journal of the Franklin Institute, August 1948, pp 123-148.
5. Johnson, E. D., et. al. "Secure Program System Evaluation Code Under Radiation Environment (U) - Final Report Report," (This work was supported by the Defense Atomic Support Agency, Washington, D. C. and Distribution limited to U.S. Government Agencies only; Test and Evaluation; Other requests for this document must be referred to Director, Defense Nuclear Agency, Washington, D.C.), Autonetics Pub. #DASA 2802, C70/703/501. (Prepared under DASA Contract No. DASA01-70-C-0080), 30 July 1971.